# Performance Analysis of Plant Monitoring Nanosensor Networks at THz Frequencies

Armita Afsharinejad, *Student Member, IEEE*, Alan Davy, Brendan Jennings, *Member, IEEE*, and Conor Brennan, *Member, IEEE*

***Abstract*—Future wireless nanosensor networks are envisioned to operate in the THz band, due to the tiny size of the network components. Among the diverse range of applications that such networks promise, high-resolution plant monitoring systems are the categories which can benefit from the size and high sensitivity of nanosensor devices and also the high bandwidth provided by them. However, communications at the THz frequency band, especially within a hybrid channel like plant foliage, undergo peculiar types of attenuation and distortion. These phenomena, which can challenge the feasibility of the aforementioned applications, need to be addressed/modeled precisely. Therefore, in this paper, we propose the first THz path-loss model within a plant environment. In addition, we provide a simplified model of plant structure as well as a model for the probability of successful transmissions between nanosensors and microscale receivers mounted on the plant stem. The introduced models consider the limited capability of THz radiation to propagate through plant leaves, and also the high free-space path-loss as the main sources of signal loss in the network communications. Furthermore, these models can be customized based on the structural characteristics of a plant, e.g., leaves size and distribution, to account for a variety of plant species. Finally, the performance of communications based on the provided models is evaluated for different network scenarios.**

***Index Terms*—High-resolution plant monitoring, path-loss model, THz communications, wireless nanosensor networks (WNSNs).**

## I. Introduction

THE TINY dimensions of the nanosensor devices allow them to be embedded in various objects and devices in our environment to obtain fine-grained data from hard-to-reach locations and thereby enabling a myriad of novel applications in industrial, biomedical, and agricultural settings [2], [3], [4]. Researchers envisage nanosensors fabricated from Carbon nanotubes that can act as highly accurate chemical sensors [5]. Moreover, a graphene-based nanoantenna can be integrated into the structure of the nanosensor device; such antennas radiate in an extremely high frequency band in the THz region, 0.3–10 THz [6], [7].

One promising deployment scenario for nanosensors is for high-resolution agricultural crop monitoring [8]–[10]. It is known that plants emit an extensive set of chemical compounds above and below the ground, providing a means of communication through which they share vital information about their surrounding environment, e.g., available resources or insect attacks [11]–[13]. For example, in the case of detecting an insect attack, some plant species emit various volatile organic compounds (VOCs) with different concentrations, based on the insect type. These emissions seek to attract the natural predators of the attacking insects as well as activating/strengthening other plants' defense systems [14]–[16].

In previous work [10], [17], we proposed a crop monitoring application of nanosensors, for detection of emitted VOCs. Our approach centers around the creation of a wireless nano sensor network (WNSN) wherein numerous nanosensors deployed on plant leaves communicate with a microscale gateway device attached to the plant stem. Although WNSN communications in the THz band can take advantage of a very high theoretical bandwidth, such transmissions are prone to very high attenuation and distortion [19]. These phenomena, which mostly depend on the transmission frequency, distance, and the medium composition, can be predicted by a precise channel model. Such a model describes the encountered path-loss, reflection, scattering, and refraction in THz communications. In the literature, there exist some THz channel models [20]–[22], but ours is the first to address the particularities of signal propagation through plant foliage.

Therefore, as the first step in this process, we propose an initial path-loss model for THz communications in the vicinity of a plant. Next, we propose an abstract model of a plant followed by a theoretical model for the calculation of the probability of successful transmissions, which can be employed for the performance analysis. This work highlights the foundation of WNSN applications in the THz channel for vegetation monitoring purposes.

In this paper, we address the specification of a path-loss model for THz communications in the vicinity of a plant and its use for the prediction of successful transmission probability. The latter is useful in the planning of the number of nanosensors to deploy to achieve a desired level of sensing capability. The contributions of this paper can be summarized as follows.

1) An enhanced THz path-loss model within plant foliage, which models the absorption loss of air molecules and

Manuscript received May 14, 2015; accepted July 27, 2015. Date of publication August 03, 2015; date of current version January 20, 2016. This work was supported by the Irish Higher Education Authority under the program for Research in Third Level Institutions (PRTLI) cycle 5, in part by the European Regional Development Fund (ERDF), via the Telecommunications Graduate Initiative (http://www.tgi.ie), and in part by the Science Foundation Ireland via the CONNECT Research Centre under Grant 13/RC/2077.

A. Afsharinejad, A. Davy, and B. Jennings are with the Telecommunication Software and Systems Group, Waterford Institute of Technology, Waterford, Ireland (e-mail: aafsharinejad@tssg.org; adavy@tssg.org; bjennings@ieee.org).

C. Brennan is with the RINCE Institute, Dublin City University, Dublin Ireland (e-mail: brennanc@eeng.dcu.ie).

Digital Object Identifier 10.1109/JIOT.2015.2463685

2327-4662 © 2015 IEEE. Personal use is permitted, but republication/redistribution requires IEEE permission.
See http://www.ieee.org/publications_standards/publications/rights/index.html for more information.

leaves, as well as the scattering loss due to leaves into account (the latter was not taken into account in our previous work [10], [17]). This model can be customized based on characteristics of particular plant species and different moisture levels in the air.

2) A simplified model of a plant structure, which can cover different plant types by varying a diverse range of parameters, e.g., size and distribution of leaves, moisture content, and so on.
3) A model for the probability of successful transmissions across WNSN deployed in plant foliage, by employing the previously mentioned models. The proposed model accounts for the limited ability of THz radiation to propagate through leaves and also the high attenuation experienced by THz waves in air.

Our earlier work [10], [17] introduced several dynamic channel allocation strategies for WNSNs communications, in order to combat the high signal attenuation. Moreover, we presented a complete analysis of the proposed strategies, by providing a basic plant and performance evaluation model. In this paper, we use a more realistic model of plant structure and, more significantly, a much enhanced path-loss model.

This paper is organized as follows. Section II reviews the existing literature in the area of THz channel models. Section III presents our system model, followed by the probability model of successful transmission in Section IV. In Section V, numerical results based on the proposed models are discussed. Finally, Section VI summarizes this paper.

## II. Related Work

Existing THz channel models characterize communication distances up to several meters [19], [23]; however, given the proximity of the components of a plant monitoring WNSN, we focus on the THz channel models for short-range transmissions. Jornet and Akyildiz [20], [24] proposed a channel model for free-space THz communications up to a few meters. The proposed model, which only considers the absorption loss due to air molecules, can be modified to accommodate various gaseous mediums with different compositions and concentrations. They show that water molecules are the main contributors of signal attenuation in free-space communications, with greater or lesser effects at distinct frequencies. As an extension to this model, the effect of particle scattering on line-of-sight (LoS) THz communications is studied and modeled in [21]. It is shown that particle scattering, which occurs due to the collision of the traveling signal with small aerosols such as water droplets, attenuates the signal and it also results in non-LoS (NLoS) propagation. The latter not only degrades the signal power but also introduces delay into communications.

Han *et al.* [22] introduced a precise THz channel model based on the ray-tracing technique, which accurately incorporates the reflection, scattering, and refraction phenomena in communications. The proposed model is validated through comparison with experimental measurements. Yang *et al.* [25] analyzed the THz path-loss in the human body for short-range communication. Through their analysis of fat and blood as body components, it is concluded that blood has a more important effect on signal degradation compared to fat. It is also shown that the effect of blood and fat on attenuating THz radiation is almost steady across the frequency band, unlike the effect of water molecules in the air. A THz path-loss model through a medium composed of human body and air is proposed by Javed and Naqvi [26]. This model takes the shadowing effect of the air molecules and body components into account, while considering short and medium transmission distances.

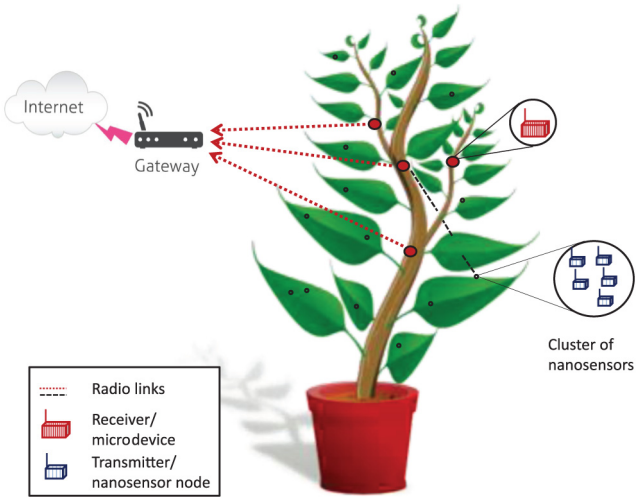


Fig. 1. Network hierarchy of a plant monitoring nanosensor network, composed of chemical nanosensors, microdevices, and a gateway.

## III. System Model

As the first step to evaluate the performance of a plant monitoring nanosensor network, we introduce our system model here. This system includes a simplified plant model as the host environment for our specific monitoring application. Furthermore, it discusses the required components and the hierarchy of the plant monitoring nanosensor network, as well as the THz channel path-loss model in such an environment.

### A. Nanosensor Nodes and the Network Model

The desired nanosensor network structure follows a hierarchical and cluster-based topology, composed of chemical nanosensor nodes, microscale devices, and network gateways (Fig. 1). Chemical nanosensor nodes are miniaturized machines that interact with their surrounding environment to detect a variety of chemical compounds emitted by plants. Microdevices are considered as control units of larger size and ample power (compared to nanosensor devices), which manage clusters of nanosensors, e.g., performing data fusion and scheduling. Finally, gateways are the interfaces that boost the applications of WNSNs by relaying the collected data from the nanonetwork to the external network/Internet. In this paper, we mainly focus on the components and specification of the nanosensor nodes, as those of microdevices and gateways are out of the scope of this discussion.

Akyildiz and Jornet [1] proposed a prototype of a nanosensor device for the first time, based on newly fabricated nanomaterials such as graphene and its derivatives. Based on the

application type, different building blocks can be integrated into the structure of a nanosensor node. Here, we assume that such a device is equipped with sensing, communication, and power blocks along with relevant processing and storage units. Here, we focus on the details of the communication units of such a nanosensor device.

The classical communication paradigms, based on metallic antennas, seem infeasible for WNSN communications due to the size and complexity of the antenna, operational frequency, and energy consumption. As a result, Akyildiz and Jornet [6] proposed a graphene-based nanoantenna as the communication unit of nanosensor devices. The maximum length of such a nanoantenna will be in the order of a few micrometers, and it will efficiently operate in the THz region, 0.3–10 THz, which is a considerably lower and more efficient frequency band compared to that of a metallic antenna of similar dimension [32]. Communications at such a high frequency can take advantage of a very high bandwidth at ultra-low latency; however, THz radiation is prone to very high degree of attenuation and distortion.

Specific communication protocols should be designed for WNSNs, which address the mentioned communication challenges. As an example, Akyildiz and Jornet [33] proposed an energy-efficient and noise-resilient modulation technique for nanosensor communications. Their proposed approach is based on ON–OFF keying (OOK), where nanosensor nodes can preserve their energy by presenting a binary status through transmitting ultra short pulses or staying silent. In [34], a novel medium access control (MAC) mechanism based on a handshaking process between communicating nanosensors is proposed. The introduced mechanism takes the energy limitations of nanosensor nodes into account, while optimizing the throughput of the WNSN communications. We introduced several frequency selection strategies in [10] and [35], where the channel allocation to nanosensors is based on optimizing the network performance. Among the proposed strategies, we showed that a two-phase frequency selection approach outperforms the rest of the strategies regarding the aggregated channel capacity and power consumption. Here, we incorporate the aforementioned modulation, MAC, and channel allocation techniques into our nanosensor communications model.

### B. Plant Structure Model

In [17], we introduced an initial abstracted model of plant structure, which can be used for network performance evaluation purposes. In the proposed structure, we assumed that a plant can be modeled as a series of concentric cylinders centered on a stem, where the number and radii of the cylinders depend on the classes of the average leaf sizes and angles in a specific plant species. Such a cylindrical model divides a plant into vertical regions, as shown in Fig. 2. In addition, we proposed the horizontal division of the plant structure into moisture regions based on the ratio of water content [36], as shown in Fig. 3.

Hence, in the most basic form, we consider the structure of a plant as $I$ concentric cylinders $C_i$ with related height and radiuses $h_i$ and $r_i$ for $i = 1, \ldots, I$. We can assume that the

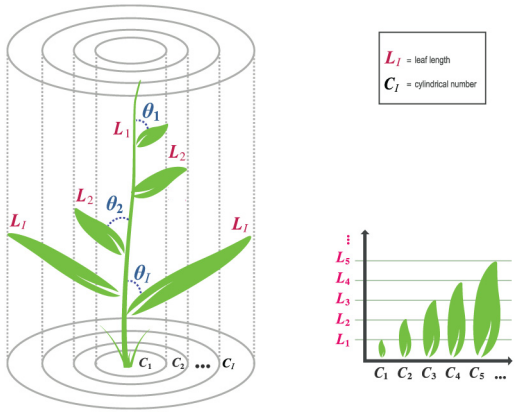


Fig. 2. Concentric cylindrical model of a plant. We assume that leaves are directly attached to the stem at a constant angle, and that leaves are one of a set number of lengths. A similar approach could be applied to plants where leaves emanate from branches (replotted from [17]).

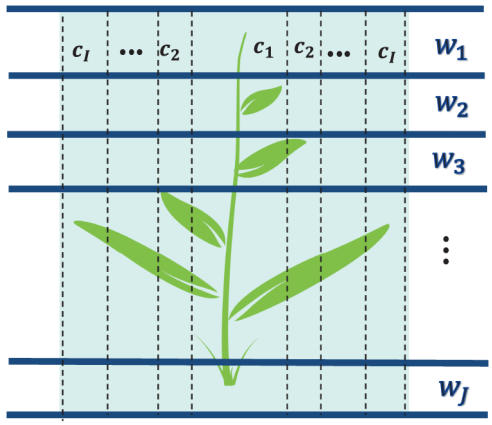


Fig. 3. Subdivision of a plant into moisture regions. The plant structure can be subdivided into horizontal moisture regions, where typically parts of the plant in regions closer to the ground contain higher moisture levels (replotted from [17]).

average leaf length $L_i$, the average leaf density/distribution (the average number of leaves per unit of distance) $\lambda_i$, and also the leaf angle $\theta_i$, are constant values within individual cylinders. We also assume that $\lambda_1 \leq \lambda_2 \leq \cdots \leq \lambda_{i-1} \leq \lambda_i$, which means that further cylinders have a higher density of leaves compared to those closer to the stem. The radius of the $i$th cylinder can be calculated as a function of the average leaf length and angle within that cylinder, i.e., $r_i = L_i \sin(\theta_i)$. As mentioned earlier, such a structure can also be divided into $J$ moisture regions with related water content $w_j$, for $j = 1, \ldots, J$. All of the described parameters in this model can be extracted through measurements of specimens of a particular plant species/variety.

It is worth noting that in [17], we considered the division of the cylindrical model into four quadrants, in which only the communicating pairs located in the same quadrant could communicate. In this paper, we consider a more realistic scenario, assuming that nodes can communicate only if they are located in the field of view of their designated microdevices.

### C. THz Path-Loss Model Within Vegetation Environment

As a signal propagates along a path, its power diminishes due to the total power being spread over a wider surface area. In addition, power is lost due to absorption and scattering from material within the propagation medium. The latter phenomena are referred to as absorption and scattering loss of a medium. Depending on the transmission distance, frequency, and also the medium composition, the severity of signal loss can vary. Hence, the total path-loss $L_{\text{tot}}(\cdot)$ for a traveling signal in the THz channel can be defined as a product of spreading loss $S(\cdot)$, absorption loss $\zeta(\cdot)$, and scattering loss $\Psi(\cdot)$, as [37]

$$L_{\text{tot}}(f,r) = S(f,r)\zeta(f,r)\Psi(f,r). \tag{1}$$

The spreading loss for omnidirectional communications can be calculated based on the Friis equation as a function of transmission distance and frequency $r$ and $f$ and the speed of light $c$ with the following definition:

$$S(f,r) = \left(\frac{4\pi f r}{c}\right)^2. \tag{2}$$

The absorption loss of a medium can be defined based on the transmittance of the medium $\tau$, i.e., the fraction of the wave that can pass through the transmission path [20]. This parameter can be defined based on the Beer–Lambert law as

$$\begin{aligned} \zeta(f,r) &= \frac{1}{\tau} \\ \tau &= \frac{P_t}{P_i} = e^{-\alpha(f)r} \end{aligned} \tag{3}$$

where $P_t$ and $P_i$ are, respectively, the radiated and incident wave powers and $\alpha(\cdot)$ is the absorption coefficient of the medium. In free-space transmissions, this parameter is calculated based on the absorbency of gaseous components of a medium such as air. Although, in a practical scenario, the transmission medium is composed of gaseous and solid materials, which absorb the incident wave differently. Considering THz propagation through vegetation, where the medium is composed of air and leaves, the total absorption coefficient can be defined as

$$\alpha(f) = A\alpha_a(f) + B\alpha_l(f). \tag{4}$$

In this definition, $A$ and $B$ are weighting coefficients, which account for the ratio of the total path traveled by the wave through the air and leaves, while $\alpha_a(f)$ and $\alpha_l(f)$ are the absorption coefficients of the air and leaves, respectively. The weighting coefficients can be calculated as

$$\begin{aligned} &A = \frac{r_a}{r} \quad B = \frac{r_l}{r} \quad r_l \approx nT \\ &\text{s.t.} \\ &r = r_a + r_l \end{aligned} \tag{5}$$

where $n$ is the average number of leaves between transmitter and receiver, $T$ is the average thickness of leaves, and $r$ is the total path length, which in turn is the sum of $r_a$ and $r_l$, the path length through air and leaves, respectively. It should be noted that $n$ is random in practice and depends on the statistical distribution of leaves in a specific plant type. In addition, by considering the thickness of a leaf in the order of a few hundred micrometers [38], the magnitude of the total traveled path by the wave through leaves can be considered negligible compared to the traveled path through the air, i.e., $B$ compared to $A$. Nevertheless, despite the small value, the magnitude of B still can affect the signal attenuation considerably.

The absorption coefficient of air $\alpha_a(\cdot)$ determines the signal attenuation caused by collision with air molecules. In [20], this coefficient is defined based on the radiative transfer theory and by means of the data provided in the HITRAN database [39]. It is shown that the magnitude of the air absorption coefficient depends on the particular mixture and concentration of the gases found in the air and it can be calculated as the sum of absorption coefficients of individual gases $\alpha_i(\cdot)$ as

$$\alpha_a(f) = \sum_i \alpha_i(f). \tag{6}$$

Further detail for calculating of individual absorption coefficients can be found in [20]. The absorption coefficient of the leaves $\alpha_l(\cdot)$ depends on their electrical properties and it can be calculated as a function of leaves extinction coefficient $\kappa_l(\cdot)$ as

$$\alpha_l(f) = \frac{4\pi\kappa_l(f)f}{c}. \tag{7}$$

The extinction coefficient determines the signal loss while it travels through the medium and is a function of the relative complex permittivity of the medium $\epsilon(\cdot)$ with the following definition [25]:

$$\begin{aligned} &\kappa_l(f) = \sqrt{\frac{\sqrt{\epsilon_1^2(f) + \epsilon_2^2(f)} - \epsilon_1(f)}{2}} \\ &\text{s.t.} \\ &\epsilon(f) = \epsilon_1(f) + i\epsilon_2(f) \end{aligned} \tag{8}$$

where $\epsilon_1(\cdot)$ and $\epsilon_2(\cdot)$ are the real and imaginary parts of the relative complex permittivity. According to the effective medium theory (EMT), the complex permittivity of a multicompound material can be described as a function of the permittivity of the individual components of the material. On the other hand, in the plant biology literature, it is stated that among different constituent components of a plant, air, water, and solid plant material are the main components influencing electromagnetic radiation [40]; the latter describes components of a dried and pressed leaf. Therefore, in [38] and [41], the permittivity of a leaf is modeled as a function of the volume fraction $V_i$ and relative complex permittivity $\epsilon_i(\cdot)$ of its components as

$$\sqrt{\epsilon_l(f)} = V_s \sqrt[3]{\epsilon_s(f)} + V_w \sqrt[3]{\epsilon_w(f)} + V_a \sqrt[3]{\epsilon_a(f)} \tag{9}$$

where indices $l$, $s$, $w$, and $a$ stand for leaf, solid plant material, water, and air. The proposed model, which is validated through real measurements, can be deployed to derive the permittivity of any type of vegetation, if the permittivity of the solid plant material and also the volumetric fraction of each component of the vegetation is known. As an example, Jördens *et al.* [38]

measured the permittivity of solid plant material by means of THz time-domain spectroscopy (TDS) and used the results to approximate the complex permittivity of coffee leaves. In this work, the measured thickness of leaves varies in the range 100–220 μm and THz spectrum under study is 0.2–1.8 THz.

The last part of the proposed path-loss model is $\Psi(\cdot)$, which accounts for the signal loss due to scattering effect of components found in the transmission path. This parameter is defined as

$$\Psi(f,r) = e^{\alpha_s(f)r} \tag{10}$$

where $\alpha_s(\cdot)$ is the scattering coefficient of the medium. Here, we only consider the scattering due to the surface roughness of leaves $\alpha_{s,l}(\cdot)$, which is proportional to the fraction of the path traveled through leaves $B$ as

$$\alpha_s(f) = B\alpha_{s,l}(f) \tag{11}$$

and $\alpha_{s,l}(\cdot)$ can be described based on the Rayleigh roughness factor as follows [38]:

$$\begin{aligned}\alpha_{s,l}(f) &= \left(\Delta\epsilon(f)\frac{4\pi\sigma f\cos(\phi)}{c}\right)^2\frac{1}{T}\\ \Delta\epsilon(f) &= \sqrt{\epsilon_l(f)} - 1\end{aligned} \tag{12}$$

where $\Delta\epsilon(\cdot)$ describes the contrast in permittivity, $\sigma$ is the standard deviation of the height profile and accounts for surface roughness, $\phi$ and $f$ are the angle and frequency of incident wave, $c$ shows the speed of light, and $T$ defines the average thickness of leaves.

Finally, the proposed path-loss model can be summarized as

$$\begin{aligned}L_{\text{tot}}(f,r) &= \left(\frac{4\pi fr}{c}\right)^2 e^{\alpha(f)r}e^{\alpha_s(f)r}\\ &= \left(\frac{4\pi fr}{c}\right)^2 e^{(A\alpha_a(f)+B(\alpha_l(f)+\alpha_{s,l}(f)))r}\end{aligned} \tag{13}$$

with the total path-loss in dB being equal to

$$\begin{aligned}L_{\text{tot}}(f,r)[dB] = 20\log\left(\frac{4\pi fr}{c}\right) + 10r(A\alpha_a(f) + B(\alpha_l(f)\\ + \alpha_{s,l}(f)))\log_{10} e.\end{aligned} \tag{14}$$

## IV. Successful Transmission Probability

In general, we can consider that the successful transmission probability across a nanosensor network depends on the following criteria: 1) the energy level of the receiver; 2) the collisions between packets transmitted by interfering nanosensor devices; and 3) the ability of the THz radiation to adequately propagate through a hybrid channel composed of obstacles and air. Based on our discussion in [17], packet loss due to lack of energy at the receiver can be avoided by employing synchronized MAC layer protocols [34], [42]. In that paper, we also showed that the collisions are unlikely to happen in certain network scenarios, where there are only few nanosensors in the network and the transmission rate is low due to the energy constraints of the nanosensors. Therefore, by focusing on single-hop communications, we can define the successful transmission probability as

$$P_s(t) = \prod_{i=1}^{N}(1 - P_i^{\text{l}} l_i(t)) \tag{15}$$

where $N$ is the number of nanosensors in the network, $P_i^{\text{l}}$ is a time-independent value which determines the loss probability for individual nanosensor nodes, and $l_i(\cdot)$ indicates whether a nanosensor is active at a given time. The latter depends on the active periods of a nanosensors $T_i^{\text{a}}$ and it is defined as

$$l_i(t) = \begin{cases} 1, & \text{if } t \in T_i^{\text{a}} : \{t_1, t_2, \ldots, t_z\} \\ & \text{where } t_1 = \text{ unif}(T_1, T_2) \text{ and} \\ & t_z = t_{z-1} + \text{ unif}(T_1, T_2) \\ 0, & \text{otherwise} \end{cases} \tag{16}$$

where $\text{unif}(T_1, T_2)$ is a uniform random value in second, which accounts for the full charging duration of a nanosensor node.

In the definition of the successful transmissions in (15), we consider that nanosensor nodes will be scattered randomly on a plant for real-time monitoring of various chemical compounds emitted by plants. Therefore, there will be a failure in network communications if any of the nanosensor nodes fails to transmit its sensed data.

As stated before, the loss probability for a nanosensor node depends on the existence of an obstruction in the LoS, and also the attenuative characteristics of the THz channel. In our specific plant monitoring application, the composition of the channel and the plant structure, specifically the existence and distribution of leaves, can affect the loss probability of individual nanosensors. Therefore, by employing the introduced channel and plant models, and considering random positions for nanosensors on leaves and fixed positions for microdevices on the stem, we calculate loss probability for individual nanosensors as follows.

### A. Nanosensor Outside Field of View of Sink Node

If a nanosensor device is outside the field of view of its designated microdevice, i.e., $\omega$ in Fig. 4, the THz radiation cannot reach the microdevice. This statement is based on the assumption that the stem does not pass the high-frequency radiation due to its high volume of water content. The field of view for a microdevice can be calculated based on the depth of a microdevices $h_m$, the radius of stem $r_s$, and also the position of microdevice around the stem, as demonstrated in this figure. Therefore, the loss probability is defined as

$$P_i^{\text{l}} = 1. \tag{17}$$

### B. Nanosensor Within Field of View of Sink Node

If a nanosensor device is within the field of view of its sink node, the loss probability depends on the distance and the leaf distribution between them. To calculate such a probability, first, we are interested to know what is the maximum number of

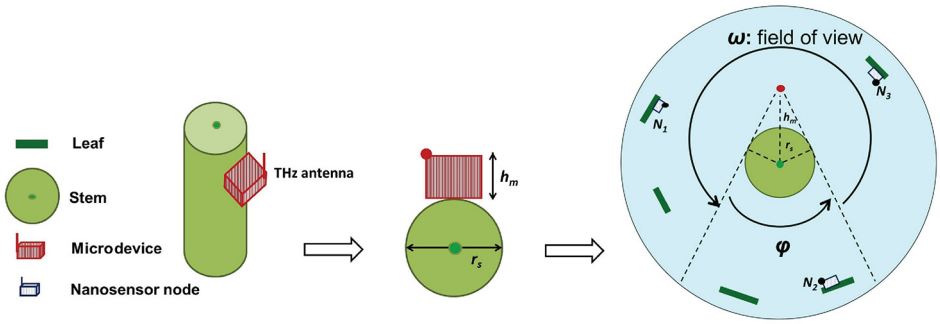


Fig. 4. Top view of the cylindrical plant model, demonstrating the field of view of a microdevice $\omega$. A nanosensor can communicate with its designated microdevice only if it is within the field of view of microdevice, assuming that THz radiation cannot pass through the stem due to its high volume of moisture content. Therefore, in this figure, $N_1$ and $N_3$ can communicate with the microdevice, while $N_2$ is obstructed by the stem.

leaves between two communicating nodes that allows the correct reception of the signal at the receiver. This in turn depends on the specific distribution of the leaves. So, we assume the path-loss threshold for nanosensor communications is $L_{\text{th}}$ dB, i.e., the maximum permitted path-loss for a correct signal demodulation process at the receiver. By replacing the desired value of the path-loss threshold in (14), and also replacing the $A$ with its equivalent from (5), the maximum proportion of the path that can occur through leaves $B_{\max}$ can be calculated as

$$B_{\max} = \frac{\frac{L_{\text{th}} - 20\log\left(\frac{4\pi f r}{c}\right)}{10r\log_{10} e} - \alpha_a(f)}{\alpha_l(f) + \alpha_{s,l}(f) - \alpha_a(f)} \tag{18}$$

where $f$ and $r$ are the transmission frequency and distance, $c$ is the speed of light, $\alpha_a(\cdot)$ and $\alpha_l(\cdot)$ are the absorption coefficients of air and leaves, and $\alpha_{s,l}(\cdot)$ is the scattering coefficient due to surface roughness of leaves.

From (5), we can see that the maximum ratio of the traveled path through leaves can also be calculated based on the average thickness of leaves $T$ and the maximum number of encountered leaves $N_{\max}$. Therefore, we can simplify the above equation as

$$N_{\max} = \frac{\left(\frac{L_{\text{th}} - 20\log\left(\frac{4\pi f r}{c}\right)}{10r\log_{10} e} - \alpha_a(f)\right) r}{(\alpha_l(f) + \alpha_{s,l}(f) - \alpha_a(f))\, T}. \tag{19}$$

This equation means that, if the number of leaves between any communicating pair is less than $N_{\max}$, the total path-loss will be less than the predefined threshold, hence the signal can be demodulated at the receiver (and conversely if the number of leaves is greater than $N_{\max}$, signal cannot be properly demodulated).

It should be highlighted that if the spreading loss is greater than the predefined path-loss threshold, the numerator in (19) and consequently $N_{\max}$ will be negative values. In such a case, the signal will be considered as lost and the loss probability is

$$P_i^{\text{l}} = 1. \tag{20}$$

To calculate the loss probability for individual nanosensors based on positive values of $N_{\max}$, we are interested to calculate the probability of having more than $N_{\max}$ leaves in a distance equal to $r$ m between communicating nodes as

$$P_i^{\text{l}} = P(k \text{ in } r \geq N_{\max}) = 1 - P(k \text{ in } r \leq N_{\max}) \tag{21}$$

where $k$ is the number of encountered leaves in the LoS communication.

In this paper, we assume that the distribution of the leaves in the aforementioned plant model follows a spatial Poisson point process. So, the probability of finding $k$ leaves in a distance equal to $r$ m between a nanosensor device, which is located in the $m$th cylinder, and its sink node is

$$P(k \text{ in } r) = \frac{(\lambda_m r)^k}{k!} e^{-\lambda_m r} \tag{22}$$

where $\lambda_m$ is the average number of leaves in (leaves/m), and it can be interpreted as the leaf density in the $m$th cylinder. The cumulative distribution function (cdf) of such a distribution is defined as

$$P(k \text{ in } r \leq K) = e^{-\lambda_m r} \sum_{i=1}^{\lfloor K \rfloor} \frac{(\lambda_m r)^i}{i!}. \tag{23}$$

Finally, by replacing the cdf of the spatial Poisson point process into (21), the loss probability of a nanosensor device can be defined as

$$P_i^{\text{l}} = 1 - e^{-\lambda_m r} \sum_{i=1}^{\lfloor N_{\max} \rfloor} \frac{(\lambda_m r)^i}{i!}. \tag{24}$$

## V. Numerical Results

We used MATLAB to analyze the network performance based on the defined plant structure and associated nanonetwork models. We consider a 1-m single stem coffee plant with the radius of 1 cm with two classes of leaf lengths equal to 0.2 and 0.3 m, and a leaf angle equal to 60°. The height of the plant can be divided into three equal regions with different moisture levels. This plant can be modeled as two concentric cylinders with the following related parameters: $h = 1\,\text{m}$, $I = 2$, $J = 3$, $L_1 = 0.2\,\text{m}$, $L_2 = 0.3\,\text{m}$, and $\theta_1 = \theta_2 = 60°$. To approximate the absorption coefficient of leaves, we used the measurement results in [38]. Here, we assume that nanosensors communicate with their associated micronodes in a single-hop fashion, over 50-GHz-wide transmission windows, which are assigned to them by means of a two-phase channel allocation mechanism [35]. We also assume that the field of view for

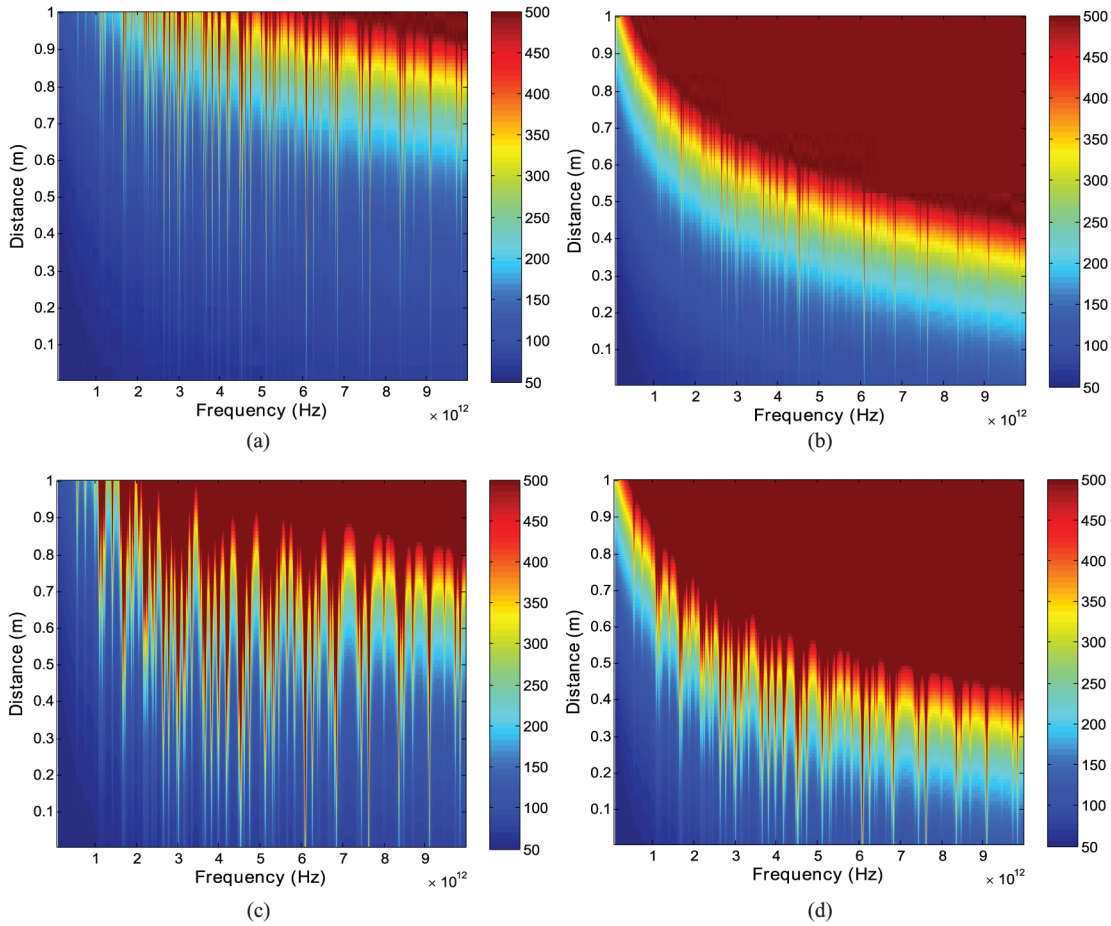


Fig. 5. Total path-loss (dB) as a function of distance and frequency, for different ratios of water content in the air and $B$, the relative proportion of path through leaves (presented results are truncated at 500 dB similar to [20]). (a) Water content $= 10\%$, $B = 0.001$. (b) Water content $= 10\%$, $B = 0.01$. (c) Water content $= 80\%$, $B = 0.001$. (d) Water content $= 80\%$, $B = 0.01$. (a) and (c) represent the path-loss in a sparse plant; (b) and (d) show that of a denser plant. The high magnitude of the path-loss decreases the effective transmission distance into a few centimeters.

microdevices is $\omega \approx 300^\circ$, given the radius of stem and the depth of a microdevice equal to $r_s = 1\,\mathrm{cm}$ and $h_m = 1\,\mathrm{cm}$, respectively.

In this section, we first evaluate the total path-loss within the plant environment for the entire THz frequency spectrum, 0.3–10 THz, and distances up to 1 m. Then, by focusing on a more practically realizable frequency range, 0.3–0.8 THz [43], and distances up to 0.5 m, we vary a combination of parameters such as water content of the medium, and the average number/thickness of leaves to analyze the performance of nanosensor communications.

### A. Path-Loss

For the first experiment, the total path-loss versus the transmission frequency and distance is presented in Fig. 5, based on (14). Here, we consider a medium composed of air and fresh coffee leaves, where the attenuation of leaves is based on the published measurement results in [38]. The published results cover a transmission range up to 1 m, as a practical transmission distance for plant monitoring nanosensor devices. We varied the moisture content of the air and also the proportion of path within the plant $B$ to study their effect on the total path-loss. In this figure, we assume a moisture content of 10% and 80% to convey two extreme conditions. In addition, we account for a sparse and a dense plant by considering $B = 0.001$ and $B = 0.01$, respectively. First, it can be observed that for a fixed ratio of water content in the air, an increase in $B$, and consequently the number of encountered leaves, causes a considerable increase in the path-loss. Therefore, the effective transmission distance is decreased greatly. Second, for a fixed value of $B$, an increase in the water content results in an increase in the path-loss at certain discrete frequencies, which is in good agreement with the results reported in [20] and [44]. Then, a comparison between all the plots shows that leaves have a higher impact on attenuating the THz radiation compared to the moisture content of the air. These observations will challenge the feasibility of plant monitoring applications of WNSN and necessitate the definition of absorption resilient transmission windows as addressed in [26] and [44].

### B. Path-Loss Threshold Definition

To evaluate the successful transmission probability across a WNSN based on (15), a value for the path-loss threshold $L_{\mathrm{th}}$ should be defined/justified. As provided before, the path-loss

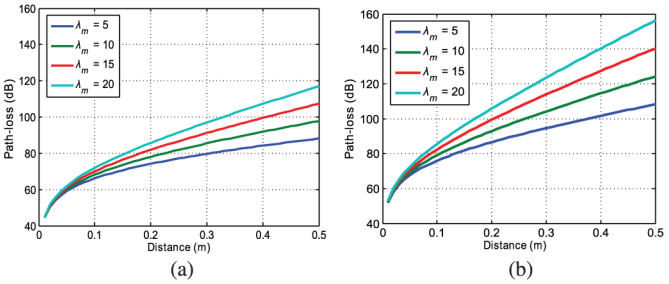


Fig. 6. Total path-loss (dB) versus distance for a variety of leaf ratios (leaves/m) and the average leaf thickness of 100 μm. (a) Best (10% water, frequency = 0.3 THz) and (b) worst (80% water, frequency = 0.8 THz) transmission conditions.

is a variable value which depends on several parameters, such as the moisture content of the transmission medium, transmission distance and frequency, and so on. Hence, we calculate the upper and lower bounds of this parameter by considering the best and the worst transmission conditions within the structural plant model. Then, we can assume that the total path-loss for the rest of the transmission conditions will fall into the defined boundaries. Here, we consider the transmission distances up to 0.5 m as the longest distance between two communicating nodes in our specific network scenario, as well as frequencies in the range of 0.3–0.8 THz. As the best condition, the transmission frequency and water content in the air are assumed as 0.3 THz and 10%; and for the worst scenario, these parameters are considered as 0.8 THz and 80%. In Fig. 6, the total path-loss versus distance is plotted for different ratios of leaves ($\lambda = 5, \ldots, 20$ [leaves/m]) and the average leaf thickness of 100 μm. Based on this figure, and also assuming that the average number of leaves per meter distance in a typical coffee plant is $\lambda$ = 15, the path-loss threshold can be considered to be in the range of 110–140 dB.

### C. Analysis of the Maximum Number of Leaves

In this section, the maximum number of leaves $N_{\max}$ based on (19) is presented by varying different parameters such as distance, frequency, and the path-loss threshold $L_{\text{th}}$. In Fig. 7, it can be observed that for 10% of moisture content, an increase in the frequency or distance results in an almost steady decrease in the number of leaves for both values of threshold, whereas, for a high moisture content equal to 80%, an increase in the frequency can result in a rapid decrease or increase in the maximum leaf number. This peculiar behavior, specifically for distances over 0.2 m, is due to the variable magnitude of molecular absorption loss at high moisture rates and random THz frequencies. To justify this claim, the total path-loss for a distance range of 0.2–0.5 m and a frequency range of 0.3–0.8 THz and variable water contents is presented in Fig. 8. As it is shown, the magnitude of the path-loss for a higher moisture content has local peaks, specifically in the range of 0.5–0.6 and 0.7–0.8 THz. When these peaks occur, there is less link budget left for attenuation by leaves and the maximum number of leaves drops accordingly (in Fig. 7), before rising again as we move away from the peak.

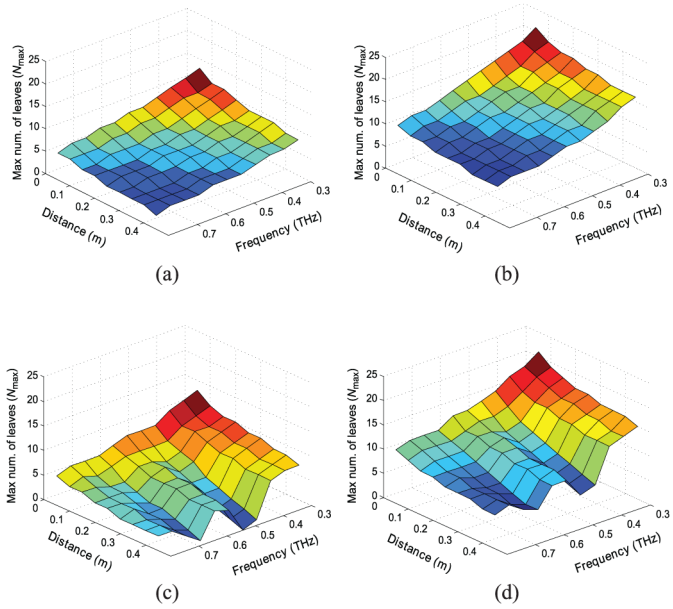


Fig. 7. Maximum number of leaves of a given channel condition, where the average leaf thickness is 100 μm, the average number of leaves is $\lambda$ = 15 (leaves/m), and path-loss thresholds are fixed values. For higher moisture ratios and longer distances, $N_{\max}$ fluctuates considerably. (a) Water content = 10%, path-loss threshold = 110 dB. (b) Water content = 10%, path-loss threshold = 140 dB. (c) Water content = 80%, path-loss threshold = 110 dB. (d) Water content = 80%, path-loss threshold = 140 dB.

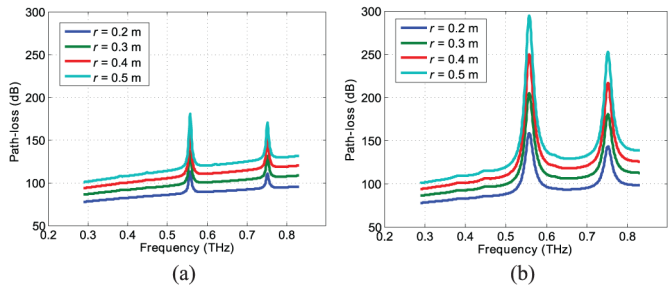


Fig. 8. Total path-loss versus distance, with an average leaf number of $\lambda$ = 15 (leaves/m) and an average leaf thickness of 100 μm. (a) Water content = 10%. (b) Water content = 80%.

In Fig. 9, the maximum number of leaves for various moisture content and transmission frequencies is plotted. In all the figures, a decrease in the maximum number of leaves can be observed as the distance increases and path-loss threshold decreases.

### D. Loss Probability for a Single Radio Link

In this section, the loss probability for a single radio link scenario based on (24) is analyzed. For such a purpose, first, the maximum number of leaves allowed in a link and under certain channel conditions is plotted in Fig. 10(a) and (b), by deploying (19). Then, based on these plots, the resulting loss probability for the same channel conditions are presented in Fig. 10(c) and (d). It can be observed that whenever the number of leaves stays constant over distance, it results in a steady increase in the related loss probability. However, whenever the number of

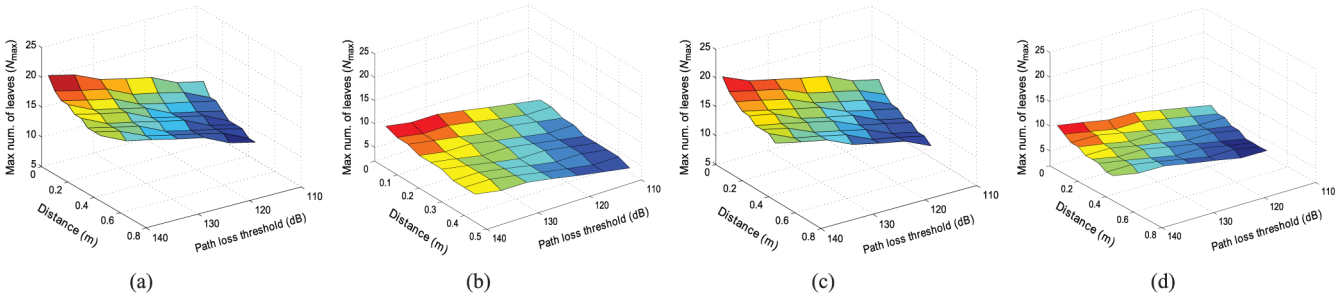


Fig. 9. Maximum number of leaves for a given channel condition, where the average leaf thickness is 100 μm, the average number of leaves is $\lambda$ = 15 (leaves/m), and transmission frequencies are fixed values. (a) Water content = 10%, frequency = 0.3 THz. (b) Water content = 10%, frequency = 0.8 THz. (c) Water content = 80%, frequency = 0.3 THz. (d) Water content = 80%, frequency = 0.8 THz. At certain distances where the number of leaves decreases, a step behavior in the related loss probability plots can be observed.

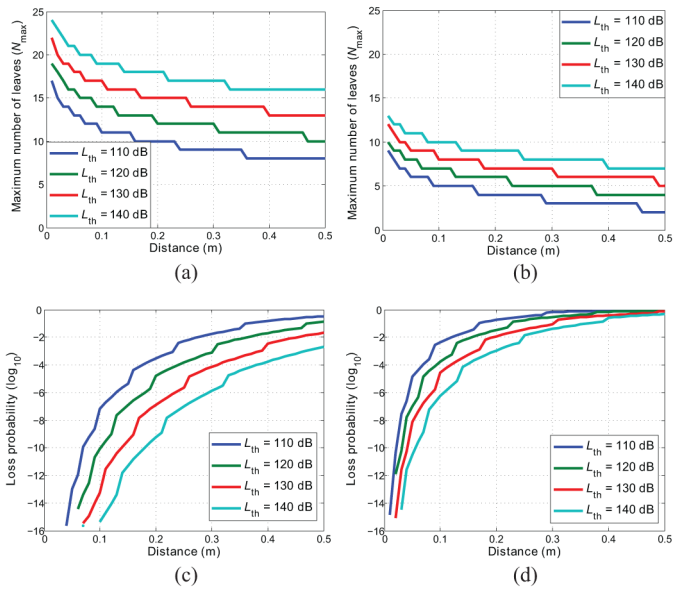


Fig. 10. Maximum number of leaves, for fixed values of frequency and moisture content, where the average leaf thickness is 100 μm and the average number of leaves is $\lambda$ = 15 (leaves/m) in (a) and (b). The resulting loss probability for a single radio link in (c) and (d). (a) Water content = 10%, frequency = 0.3 THz. (b) Water content = 80%, frequency = 0.8 THz. (c) Water content = 10%, frequency = 0.3 THz. (d) Water content = 80%, frequency = 0.8 THz. At certain distances where the number of leaves decreases, a step behavior in the related loss probability plots can be observed.

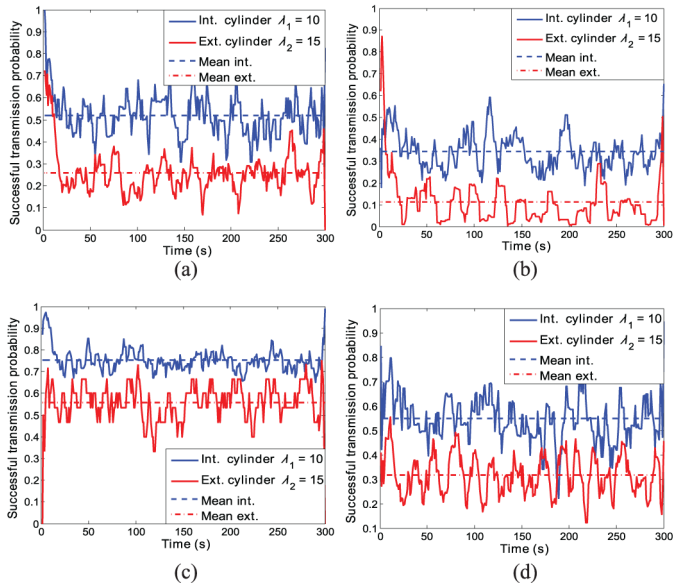


Fig. 11. Successful transmission probability for a WNSN composed of four microdevices and 100 nanosensors located evenly within the internal/external cylinders and moisture regions. (a) Leaf thickness = 100 μm, path-loss threshold = 110 dB. (b) Leaf thickness = 200 μm, path-loss threshold = 110 dB. (c) Leaf thickness = 100 μm, path-loss threshold = 140 dB. (d) Leaf thickness = 200 μm, path-loss threshold = 140 dB.

leaves changes at a given distance, it causes a step behavior in the loss probability plot. A comparison between the loss probability plots shows the high impact of the moisture content, frequency, and also the path-loss threshold on the effective transmission distance.

### *E. Successful Transmission Probability of the Nanosensor Network*

In order to study the successful transmission probability across a plant monitoring WNSN, we simulated the plant model with the aforementioned specifications. In this simulation model, the height of the plant is divided into three moisture regions with 10%, 40%, and 80% water content, respectively, and it is also vertically divided into two cylindrical regions. We deployed 4 microdevices and 100 nanosensors, which are evenly distributed between 2 cylinders and moisture regions, to monitor the emitted chemicals by the plant. We assume that the average numbers of leaves in the internal and external cylinders are $\lambda_1 = 10$ and $\lambda_2 = 15$ (leaves/m). In Fig. 11, the successful transmission probability in each cylinder is presented based on (15), and for different values of the path-loss threshold and the average leaf thickness. The provided results are averaged over 10-s periods. It is worth noting that (15) is a function of time and it varies based on the number of active nanosensor nodes, and their channel conditions. We assume that after depleting the energy, it takes nanosensors a random time in the range 50–60 s to be fully charged and capable to communicate [28]. Therefore, at any given time, there will be only a small number of active nanosensors in the network.

A comparison between all the plots shows a higher probability of success in transmissions for the nanosensors located in the internal cylinder, due to a lower ratio of leaves in this region.

Then, it can be observed that for a certain value of the average leaf thickness, increasing the path-loss threshold results in a greater increase in the successful transmission probability of the nanosensors located in the external cylinder, compared with those which are located in the internal cylinder. This observation is due to a shorter distance between nanosensors located in the internal cylinder and their sink nodes, as well as the lower ratio of the leaves in the internal cylinder. Based on the same reason, for a given path-loss threshold, increasing the average leaf thickness affects communications in the external cylinder more considerably compared to that of the internal cylinder.

## VI. Conclusion

In view of future THz band nanosensor networks, we proposed high-resolution plant monitoring systems as a potential application. Such systems can provide the research community with insights into the methods that plants communicate among themselves, as well as the types of information they exchange. Despite the sophistication of such applications, there are many challenges associated around their feasibility. Some of the main challenges can be considered as the high signal attenuation and limited signal transmissivity, due to the extremely high operational frequency.

To address these challenges, we proposed an initial THz path-loss model within a vegetation environment, which considers the THz radiation in a hybrid channel composed of air and plant leaves. To facilitate the performance analysis of communications based on this model, we also proposed a simplified plant model and a theoretical model for the probability of successful transmissions, which can accommodate different plant types. Our numerical results suggest that the density of leaves has a high and linear impact on the magnitude of the path-loss for different transmission frequencies. In contrast, the effect of moisture ratio of the air on the path-loss is variable across the THz frequency spectrum. Then, by considering a typical network condition, we defined a boundary for the path-loss threshold. The proposed boundary, which depends on the structure of the plant and the communication scenario, can be utilized for definition of the demodulation threshold at the receiver. The latter can be considered as an initial guideline for receiver design purposes.

We analyzed the effect of the structural properties of the plant and also the boundaries of the path-loss threshold, on the communications across a single radio link, as well as a network of nanosensor devices. Our analysis suggests that the plant characteristics, e.g., the thickness and density of leaves, the moisture content of the medium, transmission frequency, and also the path-loss threshold have a great impact on the performance of WNSN communications. Therefore, for network design purposes, all such parameters should be taken into account to provide the desired performance level. We believe that the provided models and analysis can form the foundation of vegetation monitoring applications of WNSNs.

As the future work, we wish to extend the presented path-loss model to include the attenuation due to fruit, stalk, and branches of plants. In addition, although our model is based on measured absorption data available in the literature for individual leaves and leaf types, we wish to validate our proposed model through comparison with some real measurements involving links operating in the vicinity of a variety of plants. The definition of a model for spatial distribution of coffee leaves, based on real measurements, can also be considered as the future work of this study. Such a model can be deployed in our proposed framework for a more accurate performance analysis of the nanonetwork communications.

## References


[1] I. Akyildiz and J. Jornet, "Electromagnetic wireless nanosensor networks," *Nano Commun. Netw.*, vol. 1, no. 1, pp. 3–19, 2010.

[2] I. F. Akyildiz and J. M. Jornet, "The Internet of Nano-Things," *IEEE Wireless Commun.*, vol. 17, no. 6, pp. 58–63, Dec. 2010.

[3] J. M. Jornet and I. F. Akyildiz, "The Internet of Multimedia Nano-Things," *Nano Commun. Netw.*, vol. 3, no. 4, pp. 242–251, 2012.

[4] S. Balasubramaniam and J. Kangasharju, "Realizing the Internet of Nano Things: Challenges, solutions, and applications," *Computer*, vol. 46, no. 2, pp. 62–68, 2013.

[5] Y. Cui, Q. Wei, H. Park, and C. M. Lieber, "Nanowire nanosensors for highly sensitive and selective detection of biological and chemical species," *Science*, vol. 293, no. 5533, pp. 1289–1292, 2001.

[6] J. Jornet and I. Akyildiz, "Graphene-based nano-antennas for electromagnetic nanocommunications in the terahertz band," in *Proc. IEEE Eur. Conf. Antennas Propag. (EuCAP)*, 2010, pp. 1–5.

[7] J. Jornet and I. Akyildiz, "Graphene-based plasmonic nano-antenna for terahertz band communication in nanonetworks," *IEEE J. Sel. Areas Commun.*, vol. 31, no. 12, pp. 685–694, Dec. 2013.

[8] H. Chen and R. Yada, "Nanotechnologies in agriculture: New tools for sustainable development," *Trends Food Sci. Technol.*, vol. 22, no. 11, pp. 585–594, 2011.

[9] R. Kumar, M. Sharon, and A. K. Choudhary, "Nanotechnology in agricultural diseases and food safety," *J. Phytol.*, vol. 2, no. 4, pp. 83–92, 2010.

[10] A. Afsharinejad, A. Davy, and B. Jennings, "Frequency selection strategies under varying moisture levels in wireless nano-networks," in *Proc. 1st Annu. Int. Conf. Nanoscale Comput. Commun. (Nanocom)*, 2014, pp. 1–9.

[11] M. Gagliano, M. Renton, N. Duvdevani, M. Timmins, and S. Mancuso, "Acoustic and magnetic communication in plants," *Plant Signal. Behav.*, vol. 7, no. 10, pp. 1346–1348, 2012.

[12] M. Heil and J. Ton, "Long-distance signalling in plant defence," *Trends Plant Sci.*, vol. 13, no. 6, pp. 264–272, 2008.

[13] I. T. Baldwin and J. C. Schultz, "Rapid changes in tree leaf chemistry induced by damage: Evidence for communication between plants," *Science*, vol. 221, pp. 277–9, 1983.

[14] P. W. Paré and J. H. Tumlinson, "Plant volatiles as a defense against insect herbivores," *Plant Physiol.*, vol. 121, no. 2, pp. 325–332, 1999.

[15] M. Heil and J. C. S. Bueno, "Within-plant signaling by volatiles leads to induction and priming of an indirect plant defense in nature," *Proc. Nat. Acad. Sci.*, vol. 104, no. 13, pp. 5467–5472, 2007.

[16] C. M. Pieterse and M. Dicke, "Plant interactions with microbes and insects: from molecular mechanisms to ecology," *Trends Plant Sci.*, vol. 12, no. 12, pp. 564–569, 2007.

[17] A. Afsharinejad, A. Davy, and B. Jennings, "Dynamic channel allocation in electromagnetic nanonetworks for high resolution monitoring of plants," *Nano Commun. Netw.*, 2015, to be published.

[18] C. A. Ryan, "Protease inhibitors in plants: Genes for improving defenses against insects and pathogens," *Annu. Rev. Phytopathol.*, vol. 28, no. 1, pp. 425–449, 1990.

[19] R. Piesiewicz *et al.*, "Short-range ultra-broadband terahertz communications: Concepts and perspectives," *IEEE Antennas Propag. Mag.*, vol. 49, no. 6, pp. 24–39, Dec. 2007.

[20] J. Jornet and I. Akyildiz, "Channel modeling and capacity analysis for electromagnetic wireless nanonetworks in the terahertz band," *IEEE Trans. Wireless Commun.*, vol. 10, no. 10, pp. 3211–3221, Oct. 2011.

[21] J. Kokkoniemi, J. Lehtomaki, K. Umebayashi, and M. Juntti, "Frequency and time domain channel models for nanonetworks in terahertz band," *IEEE Trans. Antennas Propag.*, vol. 63, no. 2, pp. 678–691, Feb. 2015.

[22] C. Han, A. Bicen, and I. Akyildiz, "Multi-ray channel modeling and wideband characterization for wireless communications in the terahertz band," *IEEE Trans. Wireless Commun.*, vol. 14, no. 5, pp. 2402–2412, May 2015.

[23] R. Piesiewicz, T. Kleine-Ostmann, N. Krumbholz, D. Mittleman, M. Koch, and T. Kürner, "Terahertz characterisation of building materials," *Electron. Lett.*, vol. 41, no. 18, pp. 1002–1004, 2005.
[24] J. M. Jornet and I. F. Akyildiz, "Channel capacity of electromagnetic nanonetworks in the terahertz band," in *Proc. IEEE Int. Conf. Commun. (ICC)*, 2010, pp. 1–6.
[25] K. Yang, A. Alomainy, and Y. Hao, "In-vivo characterisation and numerical analysis of the THz radio channel for nanoscale body-centric wireless networks," in *Proc. Joint Radio Sci. Meeting/AP-S Symp.*, 2013, pp. 218–219.
[26] I. Javed and I. Naqvi, "Frequency band selection and channel modeling for WNSN applications using simplenano," in *Proc. IEEE Int. Conf. Commun. (ICC)*, 2013, pp. 5732–5736.
[27] Y. Ohno, K. Maehashi, and K. Matsumoto, "Chemical and biological sensing applications based on graphene field-effect transistors," *Biosensors Bioelectron.*, vol. 26, no. 4, pp. 1727–1730, 2010.
[28] J. Jornet and I. Akyildiz, "Joint energy harvesting and communication analysis for perpetual wireless nanosensor networks in the terahertz band," *IEEE Trans. Nanotechnol.*, vol. 11, no. 3, pp. 570–580, May 2012.
[29] S. Roundy, "On the effectiveness of vibration-based energy harvesting," *J. Intell. Mater. Syst. Struct.*, vol. 16, no. 10, pp. 809–823, 2005.
[30] Z. Wang, "Towards self-powered nanosystems: From nanogenerators to nanopiezotronics," *Adv. Funct. Mater.*, vol. 18, no. 22, pp. 3553–3567, 2008.
[31] C. Baker, "Measurements of the natural frequencies of trees," *J. Exp. Botany*, vol. 48, no. 5, pp. 1125–1132, 1997.
[32] I. Llatser, C. Kremers, A. Cabellos-Aparicio, J. M. Jornet, E. Alarcón, and D. N. Chigrin, "Graphene-based nano-patch antenna for terahertz radiation," *Photon. Nanostruct.-Fund. Appl.*, vol. 10, no. 4, pp. 353–358, 2012.
[33] J. Jornet and I. Akyildiz, "Femtosecond-long pulse-based modulation for terahertz band communication in nanonetworks," *IEEE Trans. Commun.*, vol. 62, no. 5, pp. 1742–1754, May 2014.
[34] J. M. Jornet, J. Capdevila Pujol, and J. Solé Pareta, "Phlame: A physical layer aware MAC protocol for electromagnetic nanonetworks in the terahertz band," *Nano Commun. Netw.*, vol. 3, no. 1, pp. 74–81, 2012.
[35] A. Afsharinejad, A. Davy, B. Jennings, and S. Balasubramaniam, "GA-based frequency selection strategies for graphene-based nanocommunication networks," in *Proc. IEEE Int. Conf. Commun. (ICC)*, 2014, pp. 3642–3647.
[36] A. I. Zygielbaum, A. A. Gitelson, T. J. Arkebauer, and D. C. Rundquist, "Non-destructive detection of water stress and estimation of relative water content in maize," *Geophys. Res. Lett.*, vol. 36, no. 12, 2009, Article ID: L12403.
[37] A. Afsharinejad, A. Davy, B. Jennings, and C. Brenann, "An initial path-loss model within vegetation in the THz band," in *Proc. Eur. Conf. Antennas Propag. (EuCAP)*, 2015, to be published.
[38] C. Jördens, M. Scheller, B. Breitenstein, D. Selmar, and M. Koch, "Evaluation of leaf water status by means of permittivity at terahertz frequencies," *J. Biol. Phys.*, vol. 35, no. 3, pp. 255–264, 2009.
[39] L. S. Rothman *et al.*, "The HITRAN 2008 molecular spectroscopic database," *J. Quant. Spectrosc. Radiat. Transfer*, vol. 110, no. 9, pp. 533–572, 2009.
[40] F. T. Ulaby and R. Jedlicka, "Microwave dielectric properties of plant materials," *IEEE Trans. Geosci. Remote Sens.*, vol. GRS-22, no. 4, pp. 406–415, Jul. 1984.
[41] R. Gente *et al.*, "Determination of leaf water content from terahertz time-domain spectroscopic data," *J. Infrared Millim. Terahertz Waves*, vol. 34, nos. 3–4, pp. 316–323, 2013.
[42] S. Mohrehkesh and M. C. Weigle, "RIH-MAC: Receiver-initiated harvesting-aware MAC for nanonetworks," in *Proc. ACM Int. Conf. Nanoscale Comput. Commun. (ACM Nanocom)*, 2014, pp. 61–69.
[43] T. Schneider, A. Wiatrek, S. Preussler, M. Grigat, and R.-P. Braun, "Link budget analysis for terahertz fixed wireless links," *IEEE Trans. Terahertz Sci. Technol.*, vol. 2, no. 2, pp. 250–256, Mar. 2012.
[44] P. Boronin, V. Petrov, D. Moltchanov, Y. Koucheryavy, and J. M. Jornet, "Capacity and throughput analysis of nanoscale machine communication through transparency windows in the terahertz band," *Nano Commun. Netw.*, vol. 5, no. 3, pp. 72–82, 2014.

**Armita Afsharinejad** (S'15) received the Bachelor's degree in computer engineering and Master's degree in information technology (IT) engineering from the Azad University of Qazvin, Qazvin, Iran, in 2005 and 2008, respectively, and is currently working toward the Ph.D. degree in computer science at the Waterford Institute of Technology (WIT), Waterford, Ireland.

Her research interests include nanoscale networks, bioinspired optimization, and THz communications.

**Alan Davy** received the B.Sc. degree in applied computing and Ph.D. degree from the Waterford Institute of Technology, Waterford, Ireland, in 2002 and 2008, respectively.

He is currently a Senior Research Fellow with the TSSG Research Center, Waterford Institute of Technology, Waterford, Ireland. He has been with TSSG since 2002. He has authored over 30 peer-reviewed publications in international conferences and journals. His research interests include networked gaming, wireless network management, bioinspired systems, and nano/molecular network communications.

**Brendan Jennings** (M'06) received the B.Eng. and Ph.D. degrees from Dublin City University, Dublin, Ireland, in 1993 and 2001, respectively.

He is currently the Head of Graduate Studies with Waterford Institute of Technology, Waterford, Ireland, where he is also active as a Senior Researcher with the Emerging Networks Laboratory, Telecommunications Software and Systems Group. Within the past three years, he has spent periods as a Visiting Researcher with KTH—Royal Institute of Technology, Stockholm, Sweden, and with EMC$^2$ Research Europe, Cork, Ireland. His research interests include network management, cloud computing, and nanoscale communications.

**Conor Brennan** (M'02) received the B.A. (Mod) degree in mathematics and Ph.D. degree in electronic engineering from Trinity College Dublin (TCD), Dublin, Ireland, in 1994 and 1998, respectively.

In 2003, he became a Lecturer with the School of Electronic Engineering, Dublin City University, Dublin, Ireland, and in 2013, become a Senior Lecturer. He has coauthored over 100 peer-reviewed papers. His research interests include numerical methods for wave propagation modeling as well as computational electromagnetics.

Dr. Brennan is a Member of the Royal Irish Academy Engineering and Computer Sciences Committee.